Direct imaging reveals stable, micrometer-scale lipid domains that segregate proteins in live cells

Alexandre Toulmay and William A. Prinz

Laboratory of Cell and Molecular Biology, National Institute of Diabetes and Digestive and Kidney Diseases, National Institutes of Health, Bethesda, MD 20892

It has been proposed that membrane rafts, which are sterol- and sphingolipid-enriched liquid-ordered (L_o) domains, segregate proteins in membranes and play critical roles in numerous processes in cells. However, rafts remain controversial because they are difficult to observe in cells without invasive methods and seem to be very small (nanoscale) and short lived, leading many to question whether they exist or are physiologically relevant. In this paper, we show that micrometer-scale, stable lipid domains formed in the yeast vacuole membrane in response to nutrient deprivation, changes in the pH of the growth medium, and other stresses. All vacuolar membrane proteins tested segregated to one of two domains. These domains formed quasi-symmetrical patterns strikingly similar to those found in liposomes containing coexisting L_o and liquid-disordered regions. Indeed, we found that one of these domains is probably sterol enriched and L_o. Domain formation was shown to be regulated by the pH-responsive Rim101 signaling pathway and may also require vesicular trafficking to vacuoles.

Introduction

The raft hypothesis proposes that the affinity of sterols for lipids with saturated acyl chains, particularly sphingolipids, drives the formation of liquid-ordered (L_o) microdomains that coexist with liquid-disordered (L_d) portions of membranes. These domains are thought to organize proteins in membranes and have been suggested to regulate numerous processes in cells, including protein trafficking, intracellular signaling, and viral budding (Simons and Ikonen, 1997; Pike, 2006; Lingwood and Simons, 2010). Rafts are proposed to form primarily in compartments enriched in sterols and sphingolipids, such as the plasma membrane (PM).

Studies using giant unilamellar vesicles (GUVs) suggest how rafts may form in cells (Schroeder et al., 1994). GUVs composed of cholesterol and two phospholipids, one of which has saturated acyl chains, form stable, micrometer-sized L_o domains that coexist with L_d regions of the membrane (Baumgart et al., 2003; Veatch and Keller, 2003; Morales-Penningston et al., 2010).

One major criticism of the raft model has been that invasive methods have been necessary to visualize them in cells. Recent studies using super resolution microscopy have suggested that rafts may be small (5–200 nm) and short lived (Eggeling et al., 2009; Owen et al., 2012b). What prevents these small domains from coalescing into large domains similar to those seen in GUVs is not known.

Here, we show that stable, large raftlike lipid domains remarkably similar to those found in GUVs can form in live cells without invasive methods.

Results and discussion

The yeast vacuole performs many of the same functions as mammalian lysosomes and also regulates intracellular pH and osmotic pressure. Growing *Saccharomyces cerevisiae* cells often contain multiple vacuoles that have multilobed shapes, but as cells enter stationary growth (Stat) phase, they usually contain one large, spherical vacuole (diameter = 1–5 µm) that occupies most of the cell (Li and Kane, 2009; Armstrong, 2010). To visualize the vacuole membrane, we used the well-established protein marker Vph1, a component of the vacuole proton pump ATPase. In growing cells, Vph1-GFP is homogeneously distributed on the vacuole membrane but is excluded from regions of the vacuole that are closely apposed to the nucleus called the nuclear–vacuole junction (NVJ; Kane, 2006; Martínez-Muñoz and Kane, 2008; Dawaliby and Mayer, 2010).

Correspondence to William A. Prinz: prinzw@helix.nih.gov

Abbreviations used in this paper: GUV, giant unilamellar vesicle; L_d, liquid disordered; L_o, liquid ordered; MβCD, methyl-β-cyclodextrin; NVJ, nuclear–vacuolar junction; PM, plasma membrane; SC, synthetic complete; Stat, stationary growth; WT, wild type.

The Rockefeller University Press $30.00
J. Cell Biol. Vol. 202 No. 1 35–44
www.jcb.org/cgi/doi/10.1083/jcb.201301039

We observed that when cells enter Stat-phase, Vph1-GFP was not evenly distributed on the vacuole membranes in most cells and instead formed several striking patterns (Fig. 1, A and B; and Video 1). We classified the domain patterns into three groups: (1) partial domains, which show a few gaps in Vph1-GFP distribution, (2) quasi-symmetrical domains, and (3) coalesced domains (Fig. 1 A). Remarkably, we found that all vacuole membrane proteins tested segregate into microdomains when cells reached Stat-phase. 12 proteins showed a similar distribution to Vph1-GFP, whereas two proteins (Gtr2p and Ivy1p), exhibited the reciprocal distribution on vacuolar membranes (Fig. S1). Coexpression of Ivy1-mCherry and Vph1-GFP in live cells in Stat-phase confirmed that Ivy1-mCherry segregates from Vph1-GFP when domains form (Fig. 1 C). Time-lapse imaging revealed that the domains were stable over many minutes but evolved slowly over the course of the 3-h experiment (Video 2 and Fig. S2 A). These results indicate that during starvation, vacuolar membrane proteins segregate into either of two visible microdomains that can coalesce to form different patterns. We ruled out that cells with vacuolar domains are dying by showing that they recover from Stat-phase (Fig. S2 B).

The patterns of vacuolar membrane proteins found here in live cells (Fig. 1) are strikingly similar to the patterns of lipid phases observed in artificial membranes (Morales-Penningston et al., 2010). Membrane domains in GUVs containing coexisting L_o and L_d phases form patterns such as dots, stripes, quasi-symmetrical shapes, and large coalesced domains (Baumgart et al., 2003; Veatch and Keller, 2003) that resemble the domains we found on vacuole membranes in live cells. The patterns of domains on GUVs depend on many parameters, including the type and concentration of lipids, presence of proteins, osmotic pressure, pH, and temperature (Morales-Penningston et al., 2010). We determined whether the microdomains we found on vacuoles are lipid domains by using the vacuole-specific lipophilic dye FM4-64 (Vida and Emr, 1995). This dye displayed patterns similar to Vph1-GFP (Fig. 2 A) and colocalized with the Vph1-GFP domain (Fig. S3 B, control). This finding suggests that the domains we observed on vacuoles are indeed lipid domains.

We wondered whether the lipid domains on vacuolar membranes are, like rafts, enriched in sterols. It has previously been shown that sterols are ~7 mol percent of the lipids in vacuoles (Schneiter et al., 1999) and are known to be important for several vacuolar functions (Kato and Wickner, 2001; Fratti et al., 2004; Dawaliby and Mayer, 2010). To assess the localization of sterols in vacuoles, we added the sterol-binding dye filipin to vacuoles obtained from cells expressing Vph1-GFP. When filipin was added to vacuoles with domains, it stained discrete regions that segregated from portions of the membrane that contained Vph1-GFP (Fig. 2 B). In contrast, no visible domains were formed when filipin was added to intact vacuoles without domains, which were obtained from growing cells (unpublished data). These findings suggest that the portions of the vacuolar membrane that lack Vph1p (which contain Ivy1p and Gtr2p) are enriched in sterols, although we cannot rule out that filipin induces domain formation.

To investigate the role of sterols in vacuolar domain formation, we reduced the amount of sterols in cells by treating them with the ergosterol biosynthesis inhibitor fenpropimorph (Marcireau et al., 1990). Fenpropimorph-treated cells had fewer visible domains on vacuole membranes than untreated cells (Fig. 2 C). It should be noted that fenpropimorph slowed but did not prevent cell growth and that cultures treated with fenpropimorph reached the same cell density as untreated ones (unpublished data). We also assessed the function of sterols in domain formation by treating vacuoles with methyl-β-cyclodextrin (MβCD), a cyclic oligosaccharide that extracts sterols from membranes. When MβCD was added to vacuoles that contained domains (obtained from Stat-phase cells), it dramatically decreased the percentage of vacuoles with domains (Fig. 2 D). In contrast, vacuolar domain formation was induced by MβCD addition to vacuoles that lacked domains (obtained from growing cells; Fig. 2 D). This was probably caused by the ability of MβCD to transfer sterols between membranes (Zidovetzki and Levitan, 2007); MβCD was added to crude cellular lysates that contained other membranes in addition to intact vacuoles and probably moved sterols from other membranes to vacuoles, inducing domain formation. Although we cannot exclude that MβCD transfers a lipid other than a sterol (Zidovetzki and Levitan, 2007), we think it is most likely that it is the ability of MβCD to bind sterols that allows it to induce vacuolar domain formation or dissipate vacuolar domains. Interestingly, we also found that ergosterol but not cholesterol supported domain formation. Cells lacking Erg1 cannot synthesize sterols and require exogenous sterol to grow. They grow at the same rate with either exogenous ergosterol or cholesterol (unpublished data). We found that *erg1Δ* cells contained vacuolar domains when they were grown with ergosterol but not cholesterol (Fig. 2 E). Together, these findings suggest that one of the vacuolar membrane domains is sterol enriched, that sterols are necessary for domain formation, and that ergosterol, but not cholesterol, supports domain formation.

If one of the vacuolar domains is sterol enriched, it may be more ordered than the other domain. To assess this, we used the lipophilic dye *FAST* DiI, which has higher affinity for L_d than L_o domains (Hammond et al., 2005; Sezgin et al., 2012). We found that this dye colocalized with the Vph1-GFP–containing domain (Fig. 3 A), suggesting the reciprocal domain, which is probably sterol enriched, is more ordered. Another indication that there is a difference in the order of the two vacuolar domains is that membrane bending was observed at the junctions of the domains both in live cells and in vitro (Fig. 3, B and C). In GUVs with two phases, line tension between the domains causes membrane bending (Baumgart et al., 2003). Thus, there may be line tension between the two vacuolar domains, perhaps caused by a difference in membrane order. To obtain further evidence that vacuole membranes contain ordered regions, we incubated purified vacuoles and other organelles with Laurdan, a membrane ordering–sensitive dye (Fig. 3 D, left; Kaiser et al., 2009, 2011; Sezgin et al., 2012). We found that PM-derived membranes were more ordered than microsomes (Fig. 3 D, right), consistent with previous findings (Kaiser et al., 2011). Vacuoles from both growing cells and from cells in Stat-phase were more ordered than microsomes, consistent with the hypothesis that vacuoles contain ordered domains.

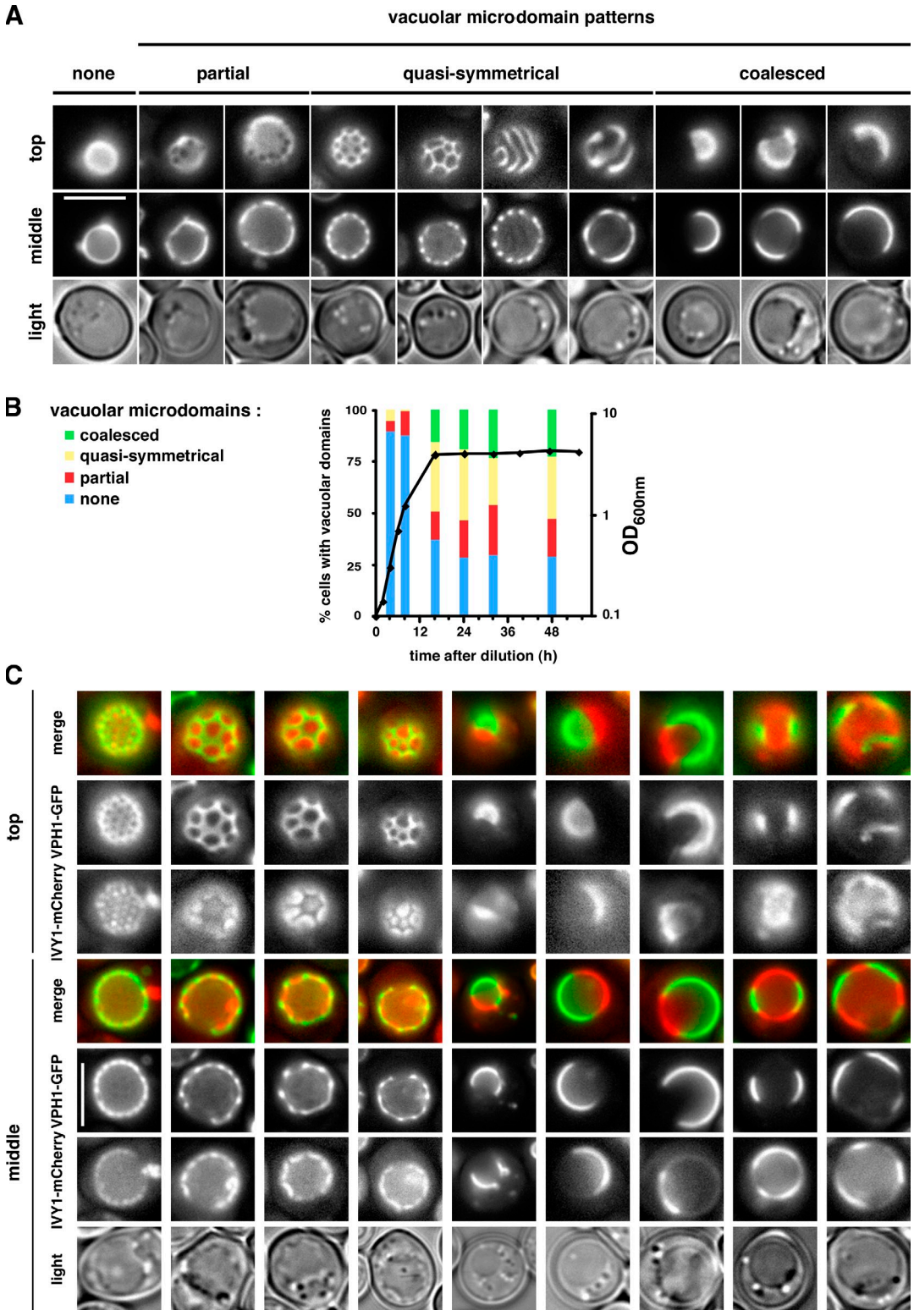

Figure 1. **Vacuole membrane proteins segregate into domains in Stat-phase.** (A) Cells expressing Vph1-GFP, in Stat-phase, were visualized live at room temperature by fluorescence microscopy focusing on either the top or middle of the vacuole. Three types of microdomains are shown: partial, quasi-symmetrical, and coalesced. (B) Cells expressing Vph1-GFP were grown in SC medium. The percentage of cells with the indicated vacuolar domain patterns and the OD_{600nm} (black line) were determined (n = 100–300 cells/time). (C) Cells expressing Vph1-GFP and Ivy1-mCherry, in Stat-phase, were visualized by fluorescent microscopy. Bars, 5 μm.

Our findings suggest that one of the vacuolar domains may be raftlike; it is sterol enriched and more ordered than the other domain. Interestingly, proteins in this domain were not resistant to cold Triton X-100 extraction (unpublished data), a hallmark of raft association (Simons and Ikonen, 1997).

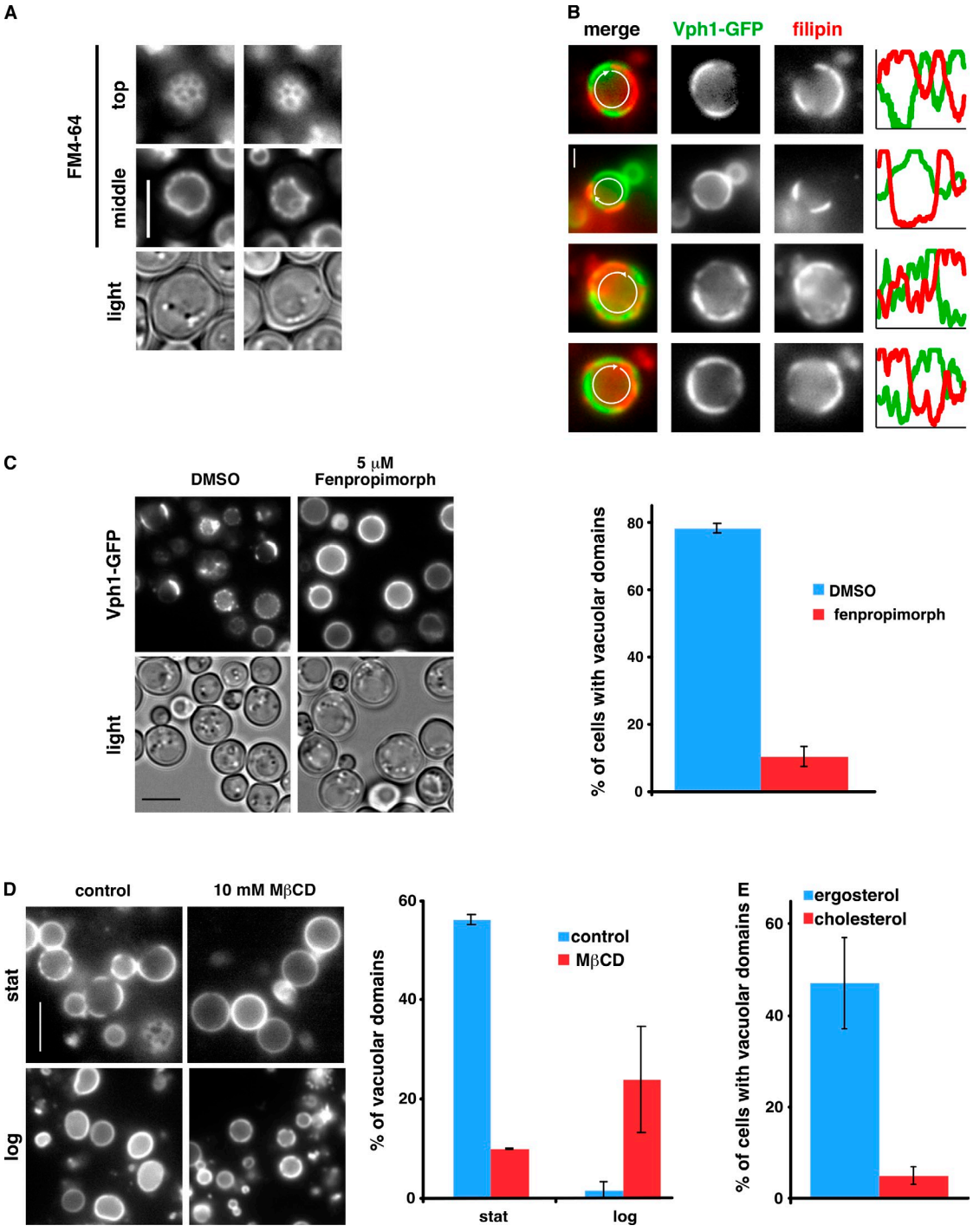

Figure 2. **Role of sterols in vacuolar domain formation.** (A) WT cells were grown in medium with FM4-64 to Stat-phase and visualized live by fluorescence microscopy. (B) Intact vacuoles from Stat-phase cells expressing Vph1-GFP were incubated with filipin for 30 min and imaged by fluorescence microscopy. Fluorescence intensities of filipin and GFP around the vacuole (arrows) were plotted. (C) 5 µM fenpropimorph or vehicle (DMSO) was added to growing cells expressing Vph1-GFP, and the cells were visualized after 16 h when they had reached Stat-phase. (D) Intact vacuoles from cells expressing Vph1-GFP were incubated with 10 mM MβCD for 30 min and imaged by fluorescence microscopy. Stat, Stat-phase; log, logarithmic growth phase. (E) Percentage of *erg1Δ* cells expressing Vph1-GFP that contained vacuoles with membrane domains when grown in YPD with ergosterol or cholesterol. The percentage of domains was calculated from 100–300 cells or vacuoles from two independent experiments. Error bars show means ± SD. Bars: (A, C, and D) 5 µm; (B) 1 µm.

We next investigated conditions that induced domain formation or caused existing domains to dissipate. Depleting cells of ATP did not cause domains to form in vacuoles that lacked domains (Fig. 4 A) or cause domains that had already formed to dissipate (not depicted), indicating that energy is not required for either process. Because it has been shown that actin and other proteins associated with the cytosolic face of the PM can drive domain formation (Kusumi et al., 1993; Douglass and Vale, 2005), we determined whether cytosolic proteins are necessary to maintain or inhibit domain formation on the vacuole. We found that the

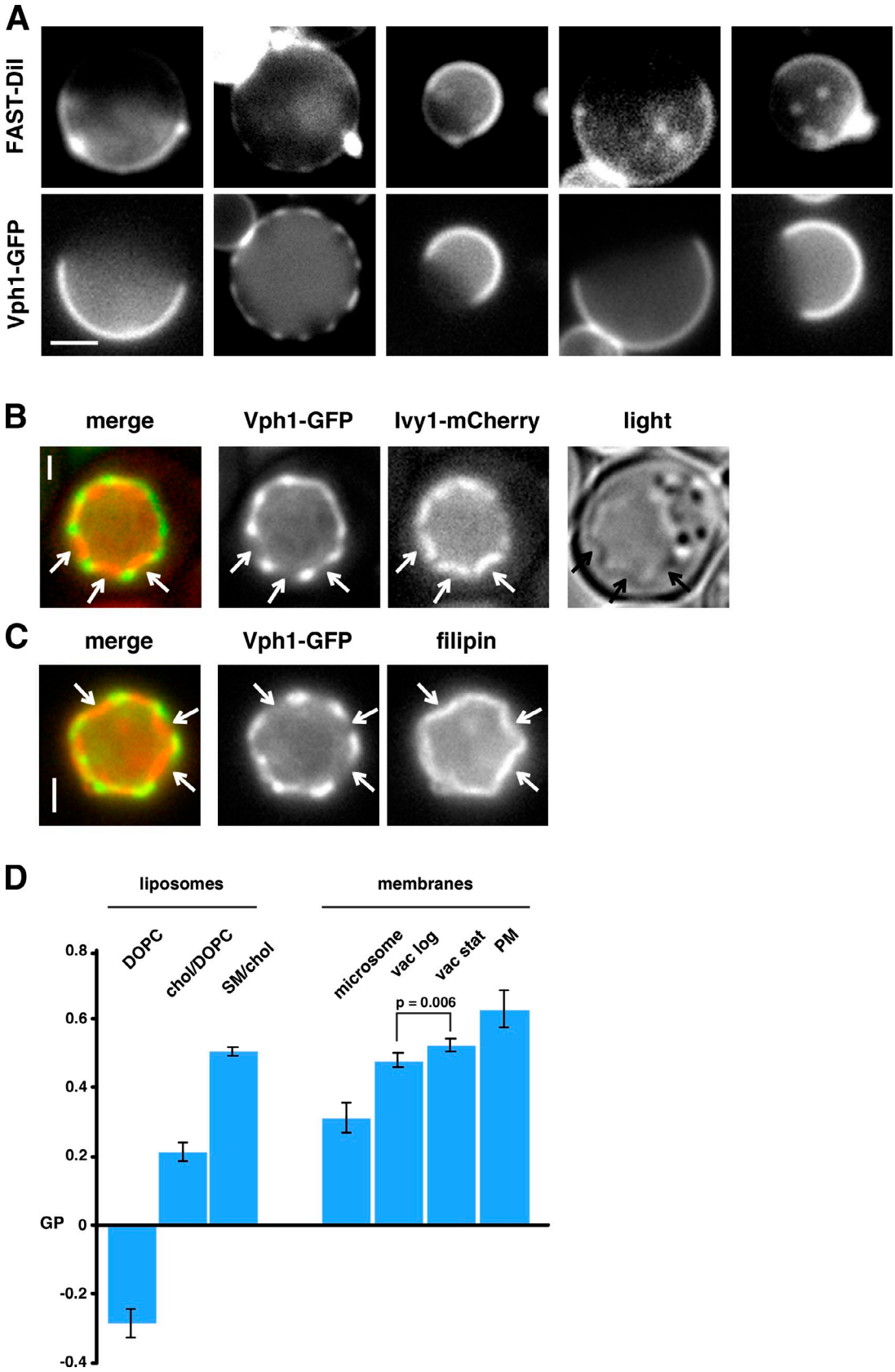

Figure 3. **Membrane ordering in the vacuolar domains.** (A) Intact vacuoles from cells expressing Vph1-GFP were incubated with *Fast* DiI for 30 min and imaged by fluorescence microscopy. (B) Images of live cells expressing Vph1-GFP and Ivy1-mCherry (shown in Fig. 1 C). (C) Images of isolated vacuoles from cells expressing Vph1-GFP and strained with filipin. In B and C, arrows indicate inward bending of sterol-enriched domains. (D) Generalized polarization (GP) of liposomes (left) and cellular membranes (right) incubated with Laurdan for 1 h at 30°C (means ± SD, n = 4–5 independent experiments). chol, cholesterol; DOPC, dioleoylphosphatidylcholine; SM, sphingomyelin; vac, vacuole. Where indicated, a two-tailed t test was used to calculate p-value. Bars: (A) 2 µm; (B and C) 1 µm.

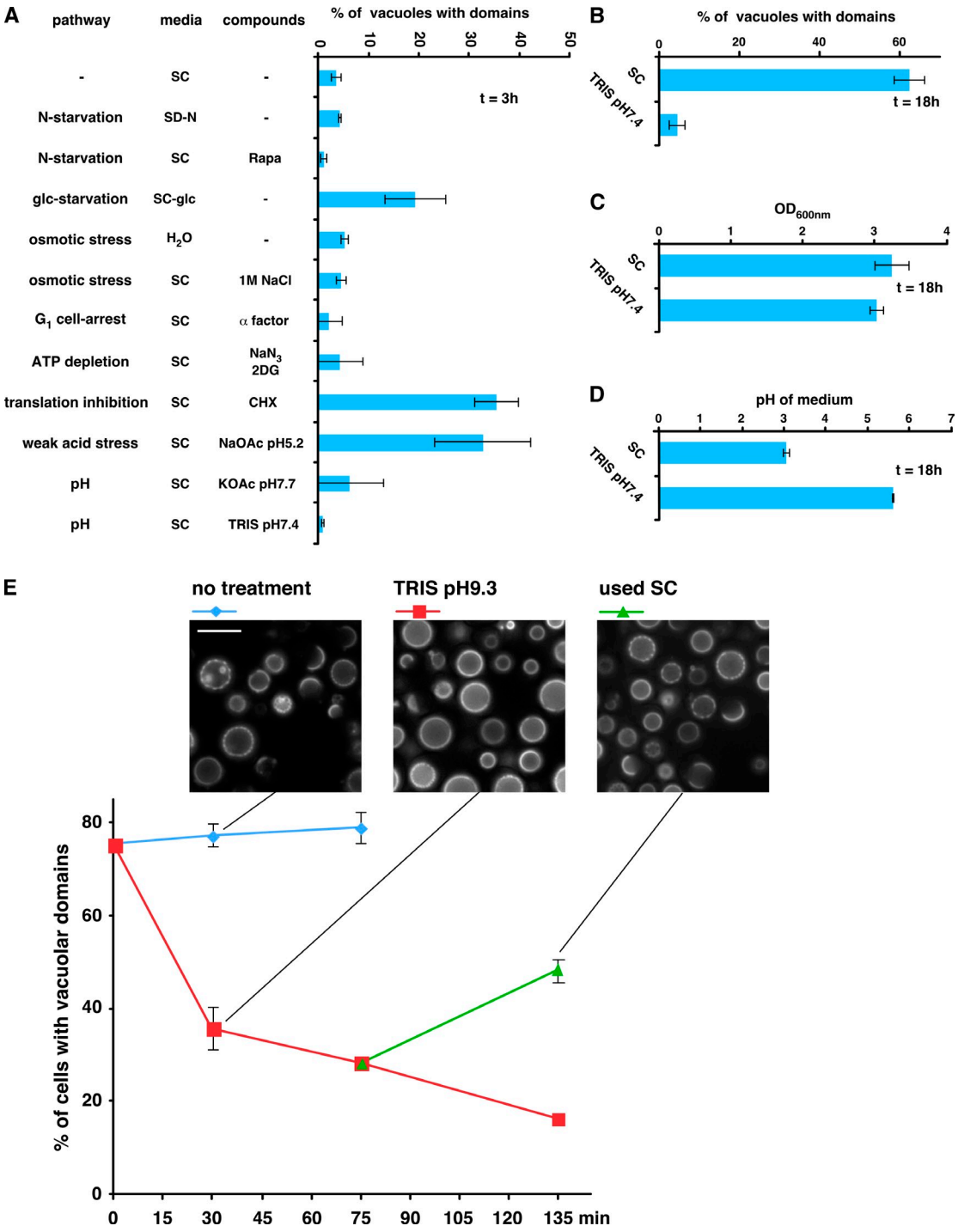

Figure 4. **Stresses that induce domain formation in vacuolar membranes.** (A) Growing cultures of cells expressing Vph1-GFP were washed and resuspended in SC, H_2O, SC lacking nitrogen (SD-N), or SC lacking glucose (SC-glc), and the indicated compounds were added (Rapa, rapamycin; 2DG, 2-deoxyglucose; CHX, cycloheximide). The percentage of cells with vacuolar domains was measured after 3 h. (B–D) The cultures in A were grown to Stat-phase (18 h), and the percentage of cells with vacuolar domains (B), the final OD_{600nm} (C), and pH (D) of the cultures were determined (n = 100–300 cells from at least two independent experiments; means ± SD). (E) pH-dependent dissipation of vacuolar domains; cells expressing Vph1-GFP were grown to Stat-phase, and the percentage of cells with vacuolar domains was determined. A portion of the cultures was pelleted, and the medium was replaced with 100 mM Tris, pH 9.3. After 75 min of incubation at 30°C, the half of the culture in Tris was pelleted and resuspended in used SC medium. Means ± SD; two independent experiments.

addition of Proteinase K to vacuoles in vitro did not induce or disrupt lipid domains on vacuole membranes (Fig. S3). Thus, cytosolic proteins and the cytosolic portions of vacuolar membrane proteins may not play a significant role in vacuolar domain formation.

To better understand how the entrance into Stat-phase induces vacuolar domain formation, we investigated the role of various stresses that occur in this growth phase: nitrogen starvation, glucose starvation, osmotic stress, cell cycle G_1 arrest, ATP

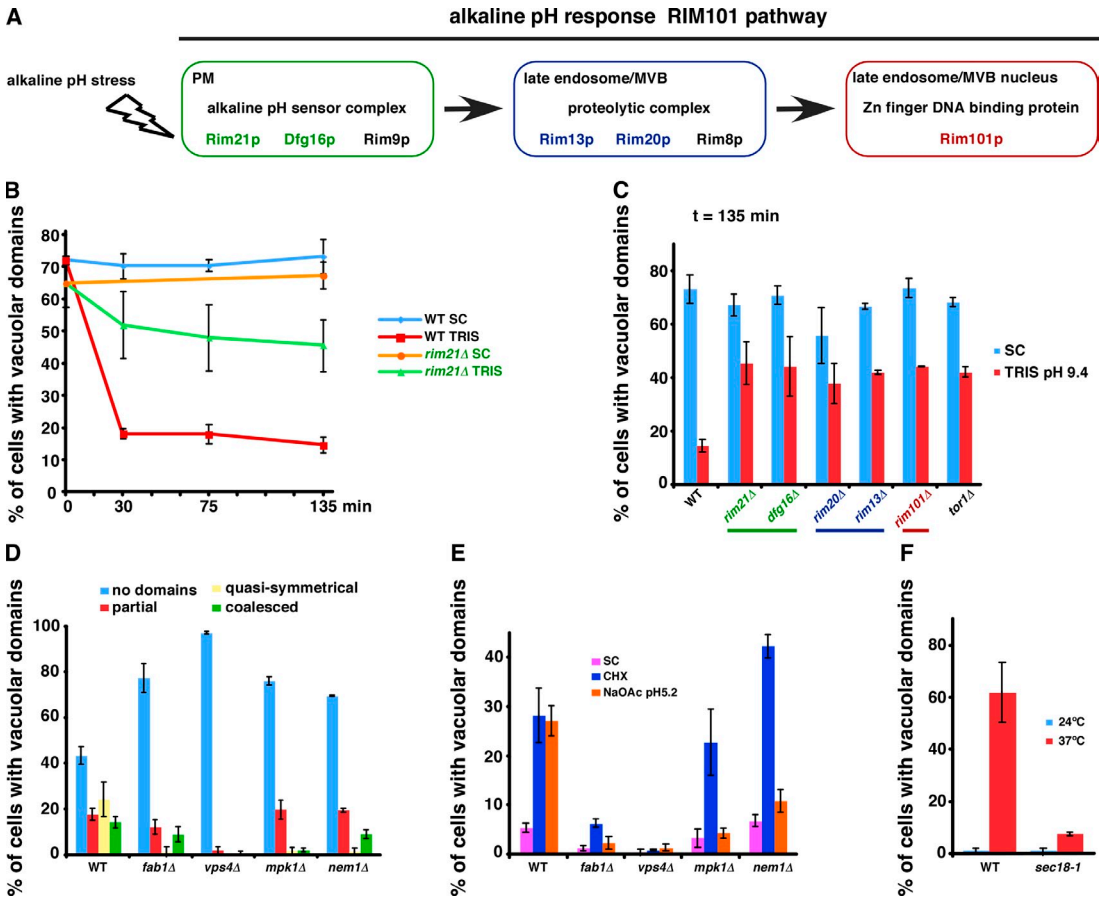

Figure 5. **Mutants that affect vacuolar domain formation or dissipation.** (A) The Rim101 pathway. (B) WT or *rim21Δ* cells expressing Vph1-GFP were grown to Stat-phase, and the percentage of cells with vacuolar domains was determined. Portions of the cultures were pelleted, and the media were replaced with 100 mM Tris, pH 9.3. (C) The indicated strains were grown as in B, and the percentage of cells with vacuolar domains was determined. (D) Percentages of vacuolar domain types in cells expressing Vph1-GFP and with the indicated genotypes were determined in Stat-phase. (E) Midlogarithmic growth–phase cultures were untreated (SC) or treated with 10 µg/ml CHX or 60 mM NaOAc, pH 5.2, for 3 h, and the percentages of cells with vacuolar domains were determined. (F) WT or *sec18-1* cells were grown at 24°C to midlogarithmic growth phase, and a portion of the cultures was shifted to 37°C for 3 h. The percentage of cells with vacuolar domains was determined. Graphs show means of 100–300 cells ± SD from two independent experiments. CHX, cycloheximide; MVB, multivesicular body.

depletion, inhibition of translation, or altering the pH of the medium. Only three of these conditions induced vacuolar domains within 3 h of addition of the compounds (Fig. 4 A). One was glucose starvation. A second was the inhibition of translation with cycloheximide, which suggests that domain formation does not require new protein synthesis but that stress signaling is likely needed. The third condition was the addition of 60 mM acetate at pH 5.2 to the medium. Interestingly, acetate at pH 7.7 did not induce domain formation (Fig. 4 A). Acetate at low pH is known to induce weak acid stress (Mollapour et al., 2008). At pHs near or below the pKa of acetate, pH 4.76, a significant fraction of acetate is protonated and can diffuse into cells. Once in the cytosol, the neutral pH causes acetate to dissociate and accumulate in cells because the acid anion cannot diffuse across the membrane, causing weak acid stress. This may be similar to what occurs in Stat-phase cultures because the pH of the medium becomes low and yeast exports acetate (Tohmola et al., 2011). Consistent with this idea, we found that buffering the medium of a growing culture to neutral pH blocked vacuolar domain formation once the culture reached Stat-phase but did not prevent cell growth (Fig. 4, B and C). We confirmed that buffering the medium prevented the acidification of the medium when cultures reached Stat-phase (Fig. 4 D), thus preventing the acidification of the medium blocked vacuolar domain formation.

Because keeping the pH of growth medium near neutral pH prevented domain coalescence, we wondered whether increasing the pH of the medium of cells that contained vacuolar domains would cause the domains to dissipate. To test this, cells were grown to Stat-phase so that ∼75% contained vacuolar domains. Replacing the medium of the cells with 100 mM Tris, pH 9.3, caused a rapid, dramatic decrease in the number of cells with vacuolar domains, and most domains that remained were partial (Fig. 4 E). Remarkably, replacement of the Tris buffer with the original used medium from the cell cultures caused domains to reform (Fig. 4 E). It should be noted that replacing the medium of a Stat-phase culture with H_2O caused no change in the percentage of cells with vacuolar domains (unpublished data). Thus, vacuolar membrane domain formation is regulated by extracellular pH.

We wanted to determine whether pH directly affects vacuolar domain formation or whether a pH-responsive signaling pathway is required. We found that incubating vacuoles in vitro

with buffers ranging from pH 6.0 to 9 did not induce domain formation or cause existing domains to dissipate (unpublished data). Thus, changes in extracellular pH probably induce a signaling event that regulates the domain formation. Consistent with this possibility, we found that the alkaline pH-responsive Rim101 pathway (Fig. 5 A; Maeda, 2012) is necessary for the dissipation of vacuolar domains when cells are in a medium with alkaline pH (Fig. 5, B and C). Interestingly, Tor1 also plays a role.

To identify other proteins that play a role in the vacuolar domain formation, we screened for mutants that fail to produce them during starvation. We selected representative mutants lacking nonessential genes with defects in the major functions of the vacuole (autophagy, vesicular trafficking, pH maintenance, and NVJ formation), lipid metabolism (sterols, sphingolipids, phospholipids, and fatty oxidation), and quiescence (the target of rapamycin and MAPK pathways). The results of the screen are shown in Table S1 and Fig. 5 D. Notably, mutants with defects in autophagy, NVJ formation, and the vacuole proton pump ATPase did not prevent domain formation (Table S1). Despite the important role of ergosterol in vacuolar domain formation, two mutants that contain ergosterol precursors as their primary sterols (*erg5Δ* and *erg6Δ*) did not have a defect in domain formation. These sterols, unlike cholesterol, are probably similar enough to ergosterol to allow domain formation. We identified four mutants that had a strong decrease in the percentage of cells with quasi-symmetrical domain patterns on the vacuole. These mutants lacked proteins involved in phosphoinositide biogenesis (*FAB1*), phospholipid homeostasis (*NEM1*), signaling linked to quiescence via the PKC pathway (*MPK1*), and vesicular trafficking to vacuoles (*VPS4*; Fig. 5 D). All four mutants also failed to form vacuolar domains when acetate, pH 5.2, was added to the medium (Fig. 5 E), confirming that these mutants cannot form lipid domains on vacuole membranes. Unexpectedly, *mpk1Δ* and *nem1Δ* still produced vacuolar lipid domains when cycloheximide was added to the medium (Fig. 5 E). Thus, weak acid stress and cycloheximide probably induce sterol-enriched domain formation by different pathways.

The results of our genetic screen confirmed that lipids (*FAB1* and *NEM1*) and signaling (*MPK1* and *NEM1*) play important roles in the formation of domains on vacuole membranes. Remarkably, the most profound defects in domain formation were found in mutants with defects in vesicular trafficking to vacuoles (*FAB1* and *VPS4*). This finding suggests that vesicular transport to vacuoles may alter the protein or lipid composition of the vacuole membrane so that domain formation is compromised. We investigated this further by determining whether mutants lacking either of the vacuolar SNAREs Vam3 and Vam7 had defects in domain formation. However, the vacuoles in these strains were small, and it was not possible to determine whether they contained domains (Table S1). In an alternative approach, we tested whether Sec18, which is required for most if not all vesicular trafficking, was needed for vacuolar domain formation. Sec18 is an essential protein, and we determined whether domain formation was blocked when cells with the conditional *sec18-1* allele were transferred from permissive temperature (24°C) to restrictive temperature (37°C) for 3 h. Surprisingly, we found that this heat stress induced domain formation in wild-type (WT) cells (Fig. 5 F). This finding allowed us to easily test whether domain formation is blocked in *sec18-1* cells. When these cells were subjected to temperature shift, domain formation was significantly reduced, consistent with the hypothesis that vesicular trafficking plays a role in domain formation.

Together, our findings show that vacuolar membrane proteins segregate into two large, stable membrane domains in live, unperturbed cells. One of these domains is probably sterol enriched and may be more ordered than the other. This domain is probably raftlike and similar to much smaller and more transient domains in the PM (Eggeling et al., 2009; Owen et al., 2012b). Stable lipid domains have been observed in endocytic compartments (Mukherjee and Maxfield, 2004), and large L_o domains have been found in the PM of some mammalian cells (Owen et al., 2012a), but it is not clear whether these domains are sterol enriched or have the other properties of rafts. A recent study suggested that most proteins in the yeast PM are enriched in a large number of coexisting patches and networks that partially overlap (Spira et al., 2012). In contrast, the yeast vacuole forms two well-defined domains that have distinct protein and lipid compositions. The dissimilarity of domains in the vacuole and in the PM may indicate that in vacuoles, as in GUVs, sterol–sphingolipid interactions provide the primary driving force for domain formation, whereas in the PM, protein–lipid and protein–protein interactions result in a much more complex mix of small, transient domains.

Two important questions about the vacuolar domains remain. First, what changes in vacuolar lipid or protein composition cause domain formation and dissipation? Second, what, if any, physiological role do vacuolar domains play in the cell? Our findings suggest that these domains are important for the cellular response to starvation and pH stress, but further investigation is required.

Materials and methods

Strains, growth conditions, and materials

The strains used in this study are listed in the Table S2. The GFP collection strains and mCherry plasmid were obtained from O. Cohen-Fix (National Institutes of Health, Bethesda, MD). Unless otherwise noted, all strains were grown at 30°C in synthetic complete (SC) media (2% glucose and 0.67% nitrogen base completed with an amino acid mix). The *erg1Δ* strain (ATY587) was grown in YPD (1% yeast extract, 2% peptone, and 2% glucose) containing 200 µg/ml G418 (Invitrogen) and 20 µg/ml ergosterol or cholesterol from a 2-mg/ml stock in Tween 80/ethanol (1:1). These cells were visualized in Stat-phase after 2 d of growth. Strains containing p416-IVY1-mCherry were grown in SC lacking uracil. SD-N medium contained 2% glucose and 0.67% nitrogen base completed without amino acid and ammonium sulfate. Unless otherwise noted, all the chemicals used in this study were obtained from Sigma-Aldrich.

Screen for conditions that induce domain formation

Growing cultures at an OD_{600nm} of 0.4–0.6 were washed and resuspended in SC, H_2O, or SD-N, compounds were added, and the cultures were grown for 3 or 18 h. The percentage of cells with vacuolar domains was determined by fluorescence microscopy. Compounds were added to the medium at these concentrations: 200 ng/ml rapamycin (Enzo Life Sciences), 20 µM α-factor (Zymo Research Corp.), 10 mM NaN_3, 10 mM 2-deoxyglucose, 10 µg/ml cycloheximide, and 60 mM NaOAc, pH 5.2 (Quality Biological), 60 mM KOAc, pH 7.7, and 100 mM Tris, pH 7.4.

Fluorescence microscopy

Cells were visualized live in growth media or H_2O with a microscope (BX61; Olympus), U Plan Apochromat 100×/1.35 NA lens, a camera (Retiga EX; QImaging), and iVision software (version 4.0.5; BioVision Technologies). Imaging was performed at room temperature (~22°C). Images

were cropped, and contrast and intensity were adjusted with Photoshop (version 7.0.1; Adobe). The quantification of intensity was determined with ImageJ software (version 1.38x; National Institutes of Health). It should be noted that vacuolar structures did not visibly change when samples were visualized at a range of temperatures from 20–55°C. For the time-lapse experiments for Fig. S2 B, cells were grown on agarose pads (Anwar et al., 2012). 2 µl of cell suspension was placed onto a 1-mm-thick pad made of 3% agarose and SC medium. The cells were covered with an 18-mm square coverslip, excess SC-agarose was cut off, and the edges were sealed with VALAP (equal parts Vaseline, lanolin, and paraffin) as described.

FM4-64 (Invitrogen) was used at 6 µg/ml (stock = 6 mg/ml in DMSO). Cells were added to medium with FM4-64 and grown ≥16 h until Stat-phase. Cells were washed two times with water before visualization.

Isolation of intact vacuoles by gentle lysis

Cells were pelleted (3,000 *g*), resuspended in 0.1 M Tris, pH 9.4, and 10 mM DTT, and incubated for 10 min at 30°C. The cells were washed once in spheroplast buffer (1.2 M sorbitol and 10 mM potassium phosphate, pH 7.4) and resuspended in spheroplast buffer with 1 mg/ml Zymolyase (Seikagaku) for 4 h (Stat-phase cells) or 1 h (logarithmic-phase cells) at 30°C. The spheroplasts were pelleted (3,000 *g*) for 5 min at room temperature and resuspended in lysis buffer (0.2 M sorbitol and 10 mM potassium phosphate, pH 7.4) to induce a gentle lysis of the spheroplasts without disrupting the vacuoles. The extent of lysis was determined by microscopy.

Cell lysates were incubated with 10 mM MβCD (in lysis buffer) for 30 min at room temperature. Filipin III (stock = 5 mg/ml in ethanol) was added to lysates at 0.2 mg/ml for 30 min to 1 h at room temperature in the dark. It should be noted that filipin stained a fraction of vacuoles immediately, but longer incubations were used to obtain staining of a higher proportion of vacuoles. *Fast* DiI (1,1′-dilinoleyl-3,3,3′,3′-tetramethylindocarbocyanine, 4-chlorobenzenesulfonate; Invitrogen) was added to lysates at 5.0 µg/ml (stock = 0.5 mg/ml in ethanol) and imaged immediately. 0.1 mg/ml Proteinase K (in lysis buffer) was added to lysates, which were incubated for 1 h at 30°C before visualization.

Screen for mutants with defects in vacuolar domain formation

Cultures of strains were started at an OD_{600nm} of 0.5 and grown for 8 h. The cultures were washed with water, resuspended in water, incubated at 30°C for 16 h, and visualized by fluorescence microscopy. The percentage of cells with quasi-symmetrical domains was determined and compared with that of WT cells. It should be noted that in these conditions, WT cells contained large vacuoles that allowed easy visualization and quantification of quasi-symmetrical domains and that ∼25% of WT cells contained these domains. In some cases, noted in Table S1, cells were not resuspended in water but instead grown continuously to Stat-phase in SC.

Determining membrane order with Laurdan

Liposomes were prepared by extrusion using a 0.1-µm membrane (Kaiser et al., 2011). Microsomes and PM were isolated from WT cells expressing Vph1-GFP (Zinser and Daum, 1995). The purified membranes were resuspended in liposome buffer (150 mM NaCl, 20 mM Hepes-KOH, pH 7.3, and 1 mM EDTA). Purified vacuoles were prepared from 1,000 OD_{600} units of cells. The cells were pelleted and resuspended in 25 ml of 1.2 M sorbitol, 40 mM KPO_i, pH 7.4, 10 mM DTT, 10 mM 2-doxyglucose, 10 mM NaN_3, 10 mM NaF, 2 mM PMSF, and 15 mg Zymolyase 20T (Seikagaku) and incubated for 45 min at 30°C with gentle shaking. The cells were pelleted (1,500 *g* for 5 min at 4°C), resuspended in 2 ml of 0.2-M sorbitol, 40 mM KPO_i, pH 7.4, and protease inhibitors (Roche), and mixed with 3 ml of 15% Ficoll 400 in PS buffer (0.2 M sorbitol and 20 mM Pipes-KOH, pH 6.8). 5.5 ml of this mixture was overlayed with 2.5 ml of 8% Ficoll 400 in PS, 3.5 ml of 4% Ficoll 400 in PS, and 1 ml of PS and centrifuged in a rotor (SW-40Ti; Beckman Coulter) at 30,000 rpm for 1.5 h at 4°C. Purified vacuoles were extracted from between the 4 and 0% layers. The vacuoles were dialyzed against liposome buffer for 1 h at 4°C and then overnight with fresh buffer. The purified organelles were incubated with 1 µM Laurdan (Sigma-Aldrich) at 30°C. Samples were excited at 385 nm using a photomultiplier (detector voltage set to 750 W; model 814; Photon Technology), with a 75-W Xenon short arc lamp (Ushio) as a light source. Data were collected and analyzed using the FeliX 32 software (PTI). All readings were taken as 150-µl samples in a 3-mm quartz cell (Starna Cells). Emission was measured from 400 to 550 nm in 5-nm increments, and generalized polarization (GP) was calculated: $GP = (I_{400–460} - I_{470–530})/(I_{400–460} + I_{470–530})$ (Kaiser et al., 2011). The background, calculated from buffer containing only Laurdan, was subtracted from emission values.

Online supplemental material

Fig. S1 shows that all vacuolar membrane proteins tested segregate to one of two domains when cells enter Stat-phase. Fig. S2 demonstrates that cells containing vacuolar domains are viable. Fig. S3 shows that vacuolar domains are not ablated or induced when isolated vacuoles are treated with protease. Table S1 gives the results of the screen for mutants with decreased percentage of cells with vacuolar domains in Stat-phase. Table S2 lists the strains used in this study. Video 1 shows a stack of images of cells containing vacuolar membrane domains. Video 2 shows time-lapse imaging of cells containing vacuolar membrane domains. Online supplemental material is available at http://www.jcb.org/cgi/content/full/jcb.201301039/DC1.

We thank O. Cohen-Fix, J. Hurley, T. Levine, and J. Hanover for strains and critically reading the manuscript.

This work was supported by the Intramural Research Program of the National Institute of Diabetes and Digestive and Kidney Diseases.

Submitted: 11 January 2013
Accepted: 3 June 2013

References

Anwar, K., R.W. Klemm, A. Condon, K.N. Severin, M. Zhang, R. Ghirlando, J. Hu, T.A. Rapoport, and W.A. Prinz. 2012. The dynamin-like GTPase Sey1p mediates homotypic ER fusion in *S. cerevisiae*. *J. Cell Biol.* 197:209–217. http://dx.doi.org/10.1083/jcb.201111115

Armstrong, J. 2010. Yeast vacuoles: more than a model lysosome. *Trends Cell Biol.* 20:580–585. http://dx.doi.org/10.1016/j.tcb.2010.06.010

Baumgart, T., S.T. Hess, and W.W. Webb. 2003. Imaging coexisting fluid domains in biomembrane models coupling curvature and line tension. *Nature*. 425:821–824. http://dx.doi.org/10.1038/nature02013

Dawaliby, R., and A. Mayer. 2010. Microautophagy of the nucleus coincides with a vacuolar diffusion barrier at nuclear-vacuolar junctions. *Mol. Biol. Cell*. 21:4173–4183. http://dx.doi.org/10.1091/mbc.E09-09-0782

Douglass, A.D., and R.D. Vale. 2005. Single-molecule microscopy reveals plasma membrane microdomains created by protein-protein networks that exclude or trap signaling molecules in T cells. *Cell*. 121:937–950. http://dx.doi.org/10.1016/j.cell.2005.04.009

Eggeling, C., C. Ringemann, R. Medda, G. Schwarzmann, K. Sandhoff, S. Polyakova, V.N. Belov, B. Hein, C. von Middendorff, A. Schönle, and S.W. Hell. 2009. Direct observation of the nanoscale dynamics of membrane lipids in a living cell. *Nature*. 457:1159–1162. http://dx.doi.org/10.1038/nature07596

Fratti, R.A., Y. Jun, A.J. Merz, N. Margolis, and W. Wickner. 2004. Interdependent assembly of specific regulatory lipids and membrane fusion proteins into the vertex ring domain of docked vacuoles. *J. Cell Biol.* 167:1087–1098. http://dx.doi.org/10.1083/jcb.200409068

Hammond, A.T., F.A. Heberle, T. Baumgart, D. Holowka, B. Baird, and G.W. Feigenson. 2005. Crosslinking a lipid raft component triggers liquid ordered-liquid disordered phase separation in model plasma membranes. *Proc. Natl. Acad. Sci. USA*. 102:6320–6325. http://dx.doi.org/10.1073/pnas.0405654102

Kaiser, H.J., D. Lingwood, I. Levental, J.L. Sampaio, L. Kalvodova, L. Rajendran, and K. Simons. 2009. Order of lipid phases in model and plasma membranes. *Proc. Natl. Acad. Sci. USA*. 106:16645–16650. http://dx.doi.org/10.1073/pnas.0908987106

Kaiser, H.J., M.A. Surma, F. Mayer, I. Levental, M. Grzybek, R.W. Klemm, S. Da Cruz, C. Meisinger, V. Müller, K. Simons, and D. Lingwood. 2011. Molecular convergence of bacterial and eukaryotic surface order. *J. Biol. Chem.* 286:40631–40637. http://dx.doi.org/10.1074/jbc.M111.276444

Kane, P.M. 2006. The where, when, and how of organelle acidification by the yeast vacuolar H+-ATPase. *Microbiol. Mol. Biol. Rev.* 70:177–191. http://dx.doi.org/10.1128/MMBR.70.1.177-191.2006

Kato, M., and W. Wickner. 2001. Ergosterol is required for the Sec18/ATP-dependent priming step of homotypic vacuole fusion. *EMBO J.* 20:4035–4040. http://dx.doi.org/10.1093/emboj/20.15.4035

Kusumi, A., Y. Sako, and M. Yamamoto. 1993. Confined lateral diffusion of membrane receptors as studied by single particle tracking (nanovid microscopy). Effects of calcium-induced differentiation in cultured epithelial cells. *Biophys. J.* 65:2021–2040. http://dx.doi.org/10.1016/S0006-3495(93)81253-0

Li, S.C., and P.M. Kane. 2009. The yeast lysosome-like vacuole: endpoint and crossroads. *Biochim. Biophys. Acta*. 1793:650–663. http://dx.doi.org/10.1016/j.bbamcr.2008.08.003

Lingwood, D., and K. Simons. 2010. Lipid rafts as a membrane-organizing principle. *Science*. 327:46–50. http://dx.doi.org/10.1126/science.1174621

Maeda, T. 2012. The signaling mechanism of ambient pH sensing and adaptation in yeast and fungi. *FEBS J.* 279:1407–1413. http://dx.doi.org/10.1111/j.1742-4658.2012.08548.x

Marcireau, C., M. Guilloton, and F. Karst. 1990. In vivo effects of fenpropimorph on the yeast *Saccharomyces cerevisiae* and determination of the molecular basis of the antifungal property. *Antimicrob. Agents Chemother.* 34:989–993. http://dx.doi.org/10.1128/AAC.34.6.989

Martínez-Muñoz, G.A., and P. Kane. 2008. Vacuolar and plasma membrane proton pumps collaborate to achieve cytosolic pH homeostasis in yeast. *J. Biol. Chem.* 283:20309–20319. http://dx.doi.org/10.1074/jbc.M710470200

Mollapour, M., A. Shepherd, and P.W. Piper. 2008. Novel stress responses facilitate *Saccharomyces cerevisiae* growth in the presence of the monocarboxylate preservatives. *Yeast*. 25:169–177. http://dx.doi.org/10.1002/yea.1576

Morales-Penningston, N.F., J. Wu, E.R. Farkas, S.L. Goh, T.M. Konyakhina, J.Y. Zheng, W.W. Webb, and G.W. Feigenson. 2010. GUV preparation and imaging: minimizing artifacts. *Biochim. Biophys. Acta*. 1798:1324–1332. http://dx.doi.org/10.1016/j.bbamem.2010.03.011

Mukherjee, S., and F.R. Maxfield. 2004. Membrane domains. *Annu. Rev. Cell Dev. Biol.* 20:839–866. http://dx.doi.org/10.1146/annurev.cellbio.20.010403.095451

Owen, D.M., C. Rentero, A. Magenau, A. Abu-Siniyeh, and K. Gaus. 2012a. Quantitative imaging of membrane lipid order in cells and organisms. *Nat. Protoc.* 7:24–35. http://dx.doi.org/10.1038/nprot.2011.419

Owen, D.M., A. Magenau, D. Williamson, and K. Gaus. 2012b. The lipid raft hypothesis revisited—new insights on raft composition and function from super-resolution fluorescence microscopy. *Bioessays*. 34:739–747. http://dx.doi.org/10.1002/bies.201200044

Pike, L.J. 2006. Rafts defined: a report on the Keystone Symposium on Lipid Rafts and Cell Function. *J. Lipid Res.* 47:1597–1598. http://dx.doi.org/10.1194/jlr.E600002-JLR200

Schneiter, R., B. Brügger, R. Sandhoff, G. Zellnig, A. Leber, M. Lampl, K. Athenstaedt, C. Hrastnik, S. Eder, G. Daum, et al. 1999. Electrospray ionization tandem mass spectrometry (ESI-MS/MS) analysis of the lipid molecular species composition of yeast subcellular membranes reveals acyl chain-based sorting/remodeling of distinct molecular species en route to the plasma membrane. *J. Cell Biol.* 146:741–754. http://dx.doi.org/10.1083/jcb.146.4.741

Schroeder, R., E. London, and D. Brown. 1994. Interactions between saturated acyl chains confer detergent resistance on lipids and glycosylphosphatidylinositol (GPI)-anchored proteins: GPI-anchored proteins in liposomes and cells show similar behavior. *Proc. Natl. Acad. Sci. USA*. 91:12130–12134. http://dx.doi.org/10.1073/pnas.91.25.12130

Sezgin, E., H.J. Kaiser, T. Baumgart, P. Schwille, K. Simons, and I. Levental. 2012. Elucidating membrane structure and protein behavior using giant plasma membrane vesicles. *Nat. Protoc.* 7:1042–1051. http://dx.doi.org/10.1038/nprot.2012.059

Simons, K., and E. Ikonen. 1997. Functional rafts in cell membranes. *Nature*. 387:569–572. http://dx.doi.org/10.1038/42408

Spira, F., N.S. Mueller, G. Beck, P. von Olshausen, J. Beig, and R. Wedlich-Söldner. 2012. Patchwork organization of the yeast plasma membrane into numerous coexisting domains. *Nat. Cell Biol.* 14:640–648. http://dx.doi.org/10.1038/ncb2487

Tohmola, N., J. Ahtinen, J.P. Pitkänen, V. Parviainen, S. Joenväärä, M. Hautamäki, P. Lindroos, J. Mäkinen, and R. Renkonen. 2011. On-line high performance liquid chromatography measurements of extracellular metabolites in an aerobic batch yeast (*Saccharomyces cerevisiae*) culture. *Biotechnology and Bioprocess Engineering*. 16:264–272. http://dx.doi.org/10.1007/s12257-010-0147-3

Veatch, S.L., and S.L. Keller. 2003. Separation of liquid phases in giant vesicles of ternary mixtures of phospholipids and cholesterol. *Biophys. J.* 85:3074–3083. http://dx.doi.org/10.1016/S0006-3495(03)74726-2

Vida, T.A., and S.D. Emr. 1995. A new vital stain for visualizing vacuolar membrane dynamics and endocytosis in yeast. *J. Cell Biol.* 128:779–792. http://dx.doi.org/10.1083/jcb.128.5.779

Zidovetzki, R., and I. Levitan. 2007. Use of cyclodextrins to manipulate plasma membrane cholesterol content: evidence, misconceptions and control strategies. *Biochim. Biophys. Acta*. 1768:1311–1324. http://dx.doi.org/10.1016/j.bbamem.2007.03.026

Zinser, E., and G. Daum. 1995. Isolation and biochemical characterization of organelles from the yeast, *Saccharomyces cerevisiae*. *Yeast*. 11:493–536. http://dx.doi.org/10.1002/yea.320110602